Preprints of the 21st IFAC World Congress (Virtual)
Berlin, Germany, July 12-17, 2020

Capacity Estimation of Lithium-ion Battery based on Electrochemical Model with Electrolyte Dynamics ⋆

Guangwei Chen * **Zhitao Liu** * **Hongye Su** *

* *State Key Laboratory of Industrial Control Technology, Institute of Cyber-Systems and Control, Zhejiang University, Hangzhou 310027, China (e-mail: 11832051@zju.edu.cn, ztliu@zju.edu.cn, hysu@iipc.zju.edu.cn)*

Abstract: The remaining capacity of a battery is a crucial indicator, which has significant impact on State of Charge (SoC) estimation and the safe operations of electric vehicles. In this paper, an electrochemical model considering the electrolyte dynamics is proposed to estimate the real capacity of a lithium-ion battery. The electrochemical model with electrolyte dynamics governed by several partial differential equations has the potential to accurately describe varieties of phenomenons inside the battery. Furthermore, a Pade' one-order approximation is adopted to obtain the transfer function between the boundary lithium-ion concentration and input current, then a boundary state estimator is proposed to estimate the the boundary lithium-ion concentration. After that, the least square method is used to obtain the adaptive update law for maximum concentration estimation in anode. Finally, the correctness of the aforementioned estimation methods is verified through simulation.

Keywords: lithium-ion battery, electrochemical model, capacity, electrolyte dynamics, Pade' approximation, least square method.

1. INTRODUCTION

On account of the superiorities of high energy density, low self-discharge rate and lack-of-memory property, lithium-ion battery has wide applications around our life, such as cell phones, laptops, electric vehicles and so on. However, capacity fade of the lithium-ion battery is inevitable on account of aging. According to the definition of SoC, we know that SoC is inversely proportional to the real capacity of the battery. Hence, the accuracy of capacity estimation has great impact on SoC computation.

Generally, the methods of capacity estimation can be classified into five parts: methods based on equivalent circuit model (ECM) consisting of several resistances and capacitances; methods on basis of electrochemical model which can detail and model the dynamic phenomena emerging in the battery; methods based on performances model using the physics equations which describe the relationship between capacity and physical properties; methods using analytical models with empirical fitting through measurements; data-driven based approaches. Markus Einhorn et al. propose an approach for estimating capacity which can be operated in any voltage stages and is unnecessary to discharge the cell completely, but this approach is strictly dependent of accurate SoC and the relationship between SoC and OCV obtained by ECM in [Einhorn et al.(2012)]. An approach based on half-cell open circuit voltages is used for capacity estimation, which can help derive the relationship between OCV and SoC at different ages, then look-up tables were established and utilized in [Marongiu et al.(2016)]. The method considering the Butter-Volmer kinetics in equivalent circuit model is proposed for capacity fade prediction by [Fleischer et al.(2014)], then an order reduction technique is used for efficient implementation on microprocessor. A two-state thermal model coupling ECM is leveraged for identifying the battery capacity in [Zhang et al.(2019)], and the convergence properties of estimation are analyzed. Compared with ECM, the research based on electrochemical model is relatively less. A pde'-based PDE parameters identifier was introduced to obtain accuracy capacity and the identifiability of the output equation was analyzed [Moura et al.(2014)]. [Li et al.(2018)] develop an single particle-based degradation model to estimate the SoH of battery by introducing the solid electrolyte interface layer formation, which is more accurate than those based on ECM and empirical model. In [Bizeray et al.(2019)], the identifiability of battery model based on Single Particle Model (SPM) is analyzed and parameters estimation including capacity are completed. Performance based model is created through investigating the dependency between physics properties and capacity. However, relative research is very few. [Samad et al.(2016)] studies the dependency between the surface force and capacity of the battery without using voltage and current measurement, which can improve the signal to noise ration of capacity estimation. In practice, due to the limit of computation, empirical

⋆ This work was supported in part by the National Key RD Program of China (Grant NO.2018YFA0703800), Science Fund for Creative Research Group of the National Natural Science Foundation of China (Grant NO.61621002), Nation Natural Science Foundation of China (NSFC:61873233, 61633019), Fundamental Research Funds for the Central Universities.

based method is widely used, which is more computationally inexpensive. By investigating the influences on aging of temperature and SoC, a capacity fade model on basis of Dakin's degradation approach is established for capacity estimation in [Baghdadi et al.(2016)]. [Hoog et al.(2017)] propose a capacity estimation method through a second-order differential voltage, which needs to obtain a reference voltage curve from a fresh battery for the comparison with the curve from the aging battery. A semi-empirical capacity fade model is used for SoH computation through the tests of 146 cells in [Goh et al.(2017)]. Considering the effect of internal resistance on SoH estimation, a regression model of capacity fade obtained by the analysis of capacity fade data can be used to accurately predict the remaining useful life [Guha et al.(2018)]. [Singh et al.(2019)] introduce a semi-empirical model of capacity fade for SoH estimation, which can extract the real maximum capacity of battery from the discharge curve. Data-driven based method for SoH estimation has become popular recently due to the development of intelligent algorithms. A support vector machine model is introduced to complete SoH estimation by capturing internal characteristics from collected data in [Klass et al.(2012)]. [Kim et al.(2015)] propose a rayleigh quotient-based method for capacity estimation, which considers this estimation as a problem of solving recursive total-least-squares (RTLS). Capacity fade estimation based on artificial neural networks is introduced to estimate capacity of battery and the Data is obtained by amounts of charging and discharging cycles in [Hussein et al.(2015)]. Based on the spare Bayesian learning method, relevance vector machine (RVM) is used to learn the dependency of capacity on the properties abstracted from the voltage and current measurements in [Hu et al.(2015)]. [Sung et al.(2016)] adopt a data-driven model to capture the variations in the shape of the charge curve when the battery ages and the parameters are identified by the least squares method. In [Liu et al.(2018)], a data-driven method, Gaussian process regression, is presented for capacity computation, which deals with the problem that the differentiate of data can enlarge the measurement noise. A model based on neural network in varieties of charge-states is developed, and the terminal voltage, temperature and load are input parameters [Richardson et al.(2019)]. Based on the measurable data, such as voltage, current and temperature from the battery, the relationship between capacity and those parameters is obtained by machine learning method in [Choi et al.(2019)].

In this paper, an electrochemical model considering the dynamics of liquid phase is proposed for capacity identification. Comparing with ECM and SPM, electrochemical model with electrolyte dynamics can detail the phenomenons inside battery more accurately and obtain the more precise prediction of terminal voltage. Furthermore, a Pade' one-order approximation is adopted to obtain the transfer function between the boundary lithium-ion concentration and input current, then a boundary state estimator is proposed to estimate the boundary lithium-ion concentration. After that, the least square method is used to obtain the adaptive update law for maximum concentration estimation in anode, which can help compute the maximum available capacity. Finally, simulation is implemented to verify the correctness of the aforementioned estimation methods.

The remaining parts of this paper are arranged as follows: Section. 2 presents the electrochemical model with the dynamics of liquid phase. The Pade' approximation is utilized in Section. 3 for boundary state estimation. In Section. 4, the capacity estimation is completed through the least squares method. Finally, the simulation is implemented to verify the correctness of the capacity estimation method in Section. 5.

2. ELECTROCHEMICAL MODEL WITH ELECTROLYTE DYNAMICS (SPME)

The SPM as the simplest version of Doyle Fuller Newman (DFN) model has been widely used in the area of estimation and control of lithium-ion battery. However, there are relatively few literatures using electrochemical model to estimate capacity of lithium-ion battery. Additionally, neglecting the dynamics of liquid phase in SPM is unwise because the terminal voltage computation is strictly dependent of liquid phase potential. Here, a modified model of SPM considering the dynamics of liquid phase is presented.

2.1 SPM Considering the Dynamics of Liquid Phase

The evolution of lithium in each electrode can be governed by the following partial differential equations:

$$\frac{\partial c_s^j}{\partial t} = \frac{D^j}{r_j^2}\frac{\partial}{\partial r_j}(r_j^2\frac{\partial c_s^j}{\partial r_j}). \tag{1}$$

Where, c_s^j is the lithium concentration in solid phase, r_j is the radial of spherical particle, D_s^j denotes the diffusion coefficient of electrode, j represent $+,-$ which mean anode and cathode. The equation (1) has the following Newman boundary conditions:

$$\frac{\partial c_s^j}{\partial r_j}(0,t) = 0, \frac{\partial c_s^j}{\partial r_j}(R_s^j,t) = -\frac{J^j}{D^j} \tag{2}$$

Where, $r_j = 0$ and $r_j = R_s^j$ respectively denote the center and the surface of single particle. J^j is the molar flux of lithium ion in anode/cathode which is directly related to the input current by the following expressions:

$$J^+ = \frac{-I}{a^+L^+FA}, J^- = \frac{+I}{a^-L^-FA} \tag{3}$$

Where, F is the Faraday constant, A represents the surface area of electrode which is considered as a uniform vale for anode/cathode, a^j is the specific active surface area obtained by $3\epsilon^j/R_s^j$, ϵ^j is volume fraction of active material. Next, the electrolyte diffusion equations are presented as follows:

$$\frac{\partial c_e^-}{\partial t}(x,t) = \frac{\partial}{\partial x}[D_e(c_e^-)\frac{\partial c_e^-}{\partial x}(x,t)] + \frac{(1-t_c^0)}{\epsilon_e^- FL^-}I(t) \tag{4}$$

$$\frac{\partial c_e^{sep}}{\partial t}(x,t) = \frac{\partial}{\partial x}[D_e(c_e^{sep})\frac{\partial c_e^{sep}}{\partial x}(x,t)] \tag{5}$$

$$\frac{\partial c_e^+}{\partial t}(x,t) = \frac{\partial}{\partial x}[D_e(c_e^+)\frac{\partial c_e^+}{\partial x}(x,t)] - \frac{(1-t_c^0)}{\epsilon_e^+ FL^+}I(t) \tag{6}$$

Where, c_e^-, c_e^+ and c_e^{sep} respectively denote the electrolyte concentration of lithium ion in cathode, anode and separator, D_e is the diffusion coefficient of lithium ion in liquid phase which is the function of lithium-ion concentration, t_c^0 is the transference number, ϵ_e^j is the volume fraction of electrolyte phase, L^j is the thickness of anode/cathode. The PDE (4),(5) and (6) are with the following boundary conditions:

$$\frac{\partial c_e^-}{\partial x}(0^-,t) = \frac{\partial c_e^+}{\partial x}(0^+,t) = 0 \tag{7}$$

$$\epsilon_e^- D_e(L^-)\frac{\partial c_e^-}{\partial x}(L^-,t) = \epsilon_e^{sep} D_e(0^{sep})\frac{\partial c_e^{sep}}{\partial x}(0^{sep},t) \tag{8}$$

$$\epsilon_e^+ D_e(L^+)\frac{\partial c_e^+}{\partial x}(L^+,t) = \epsilon_e^{sep} D_e(L^{sep})\frac{\partial c_e^{sep}}{\partial x}(L^{sep},t) \tag{9}$$

$$c_e(L^-,t) = c_e(0^{sep},t) \tag{10}$$

$$c_e(L^{sep},t) = c_e(L^+,t) \tag{11}$$

Where, $0^-, 0^+, 0^{sep}, L^{sep}, L^-, L^+$ denote the boundary positions.
After that, the output function of terminal voltage is derived, which is dependent of solid potential $\phi_s^{\pm}(x,t)$, that is $V(t) = \phi_s^+ - \phi_s^-$. $\phi_s^{\pm}$ can be computed as follows:

$$\phi_s^{\pm}(x,t) = \bar{\eta}^{\pm}(t) + \bar{\phi}_e^{\pm} + U^{\pm}(\bar{c}_{ss}^{\pm}(t)) + FR_f^{\pm}\bar{J}^{\pm}(t) \tag{12}$$

The first term of equation (12) is overpotential which can be obtained by the following equation:

$$\bar{\eta}^{\pm}(t) = \frac{RT}{\alpha F}\sinh^{-1}\left(\frac{\mp I(t)}{2a^{\pm}L^{\pm}\bar{i}_0^{\pm}(t)}\right) \tag{13}$$

The electrolyte potential $\phi_e^{\pm}$ are governed by the following ODE:

$$\begin{aligned}\frac{\partial \phi_e}{\partial x}(x,t) = &\frac{i_e^{\pm}(x,t)}{k(c_e)} + \frac{2RT}{F}(1-t_c^0)\\ &\times\left(1+\frac{\mathrm{d}\ln f_{c/a}}{\mathrm{d}\ln c_e}\right)\frac{\partial \ln c_e}{\partial x}(x,t)dx\end{aligned} \tag{14}$$

Where, $i_e^{\pm}$ is ionic current, $k(c_e)$ is the conductivity of electrolyte, $f_{c/a}$ denotes the mean molar activity coefficient in electrolyte. The term $(1+\frac{\mathrm{d}\ln f_{c/a}}{\mathrm{d}\ln c_e})$ is assumed as a uniform value $k_f(t)$. $\phi_e^{\pm}$ can be solved by integrating equation (14) across the battery width. Then,

$$\begin{aligned}&\bar{\phi}_e^+(0^+,t) - \bar{\phi}_e^-(0^-,t) = \frac{L^+ + 2L^{sep} + L^-}{2k(c_e)}I(t)\\ &+\frac{2RT}{F}(1-t_c^0)k_f(t)[\ln c_e(0^+,t) - \ln c_e(0^-,t)].\end{aligned} \tag{15}$$

Hence, the terminal voltage $V(t)$ can be expressed as follows

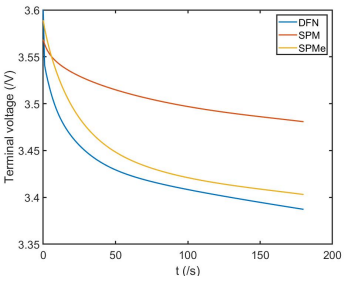

Fig. 1. Voltage predictions of DFN, SPMe and SPM

$$\begin{aligned}V(t) = &\frac{RT}{\alpha F}\sinh^{-1}\left(\frac{-I(t)}{2a^+L^+\bar{i}_0^+(t)}\right)\\ &-\frac{RT}{\alpha F}\sinh^{-1}\left(\frac{-I(t)}{2a^-L^-\bar{i}_0^-(t)}\right)\\ &+U^+(\bar{c}_{ss}^+(t)) - U^-(\bar{c}_{ss}^-(t)) - \left(\frac{R_f^+}{a^+L^+} + \frac{R_f^-}{a^-L^-}\right)I(t)\\ &+\frac{L^+ + 2L^{sep} + L^-}{2k(c_e)}I(t)\\ &+\frac{2RT}{F}(1-t_c^0)k_f(t)[\ln c_e(0^+,t) - \ln c_e(0^-,t)].\end{aligned} \tag{16}$$

Due to the introduction of electrolyte dynamics, additional two terms are generated in the last part of $V(t)$. Fig. 1 shows the terminal voltage predictions of three battery models, DFN, SPMe and SPM. DFN is the most accurate battery model which can be regarded as the true battery. We can find that the SPMe is capable of obtaining more precise voltage prediction than single SPM, which can help achieve more accurate capacity estimation.

2.2 Coordinates Normalization

For the sake of identifying the time-varying parameters, we introduce the coordinate transformation $\bar{r}_j = r_j/R_j$. The equations (1),(2) can be rewritten as follows:

$$\frac{\partial c_s^j}{\partial t} = \frac{D^j}{R_j^2}\frac{1}{\bar{r}_j^2}\frac{\partial}{\partial \bar{r}_j}\left(\bar{r}_j^2\frac{\partial c_s^j}{\partial \bar{r}_j}\right). \tag{17}$$

With the boundary conditions:

$$\frac{\partial c_s^j}{\partial \bar{r}_j}(0,t) = 0, \frac{\partial c_s^j}{\partial \bar{r}_j}(1,t) = -\frac{-R_j J^j}{D^j} \tag{18}$$

For linearizing equation (17), the coordinate transformation $w_s^j = \bar{r}_j c_s^j$ is adopted, then equations (17), (18) can be rewritten:

$$\frac{\partial w_s^j}{\partial t} = \frac{D^j}{R_j^2}\frac{\partial^2 w_s^j}{\partial \bar{r}_j^2}. \tag{19}$$

$$\frac{\partial w_s^j}{\partial \bar{r}_j}(0,t) = 0, \frac{\partial w_s^j}{\partial \bar{r}_j}(1,t) - w_s^j(1,t) = -\frac{-R_j J^j}{D^j} \tag{20}$$

Then, the overpotential equation (13) is transformed into the following expressions:

$$\bar{\eta}^+(t) = \frac{RT}{\alpha F}\sinh^{-1}\left(\frac{-I(t)}{2a^+L^+k^+\sqrt{\bar{c}_e c_{ss}^+(1-c_{ss}^+)}}\right) \tag{21}$$

$$\bar{\eta}^-(t) = \frac{RT}{\alpha F}\sinh^{-1}\left(\frac{I(t)}{2a^-L^-k^-\sqrt{\bar{c}_e c_{ss}^-(1-c_{ss}^-)}}\right) \quad (22)$$

Let

$$\begin{aligned} R_f &= \frac{R_f^+}{a^+L^+} + \frac{R_f^-}{a^-L^-}, R_e = \frac{L^+ + 2L^{sep} + L^-}{2k(c_e)}, \\ K_f &= \frac{2RT}{F}(1-t_c^0)k_f(t) \end{aligned} \quad (23)$$

Then,

$$\begin{aligned} V(t) &= \frac{RT}{\alpha F}\sinh^{-1}\left(\frac{-I(t)}{2a^+L^+k^+\sqrt{\bar{c}_e c_{ss}^+(c_{ss,max}^+ - c_{ss}^+)}}\right) \\ &-\frac{RT}{\alpha F}\sinh^{-1}\left(\frac{I(t)}{2a^-L^-k^-\sqrt{\bar{c}_e c_{ss}^-(c_{ss,max}^+ - c_{ss}^-)}}\right) \\ &+U^+(x_{ss}^+(t)) - U^-(x_{ss}^-(t)) - R_f I(t) \\ &+R_e I(t) + K_f[\ln c_e(0^+,t) - \ln c_e(0^-,t)]. \end{aligned} \quad (24)$$

3. THE PADE' APPROXIMATION FOR BOUNDARY LITHIUM-ION CONCENTRATION ESTIMATION

Introducing $\sigma_j^D = \frac{R_j^2}{D^j}$ and taking the Laplace transform of (19) yields:

$$\frac{d^2 W_s^j(\bar{r}_j, s)}{d\bar{r}_j^2} - s\sigma_j^D W_s^j(\bar{r}_j, s) = 0 \quad (25)$$

According to the boundary conditions (20) and the solution of (19) is achieved:

$$W_s^j(\bar{r}_j, s) = M^j \frac{\sinh(\bar{r}_j\sqrt{s\sigma_j^D})I(s)}{\sinh(\sqrt{s\sigma_j^D}) - \sqrt{s\sigma_j^D}\cosh\sqrt{s\sigma_j^D}} \quad (26)$$

where,$M^j = \frac{R_j}{D_s^j a^j L^j F A}$.
By substituting $w_s^j = \bar{r}_j c_s^j$ into (26), at $\bar{r}_j = 1$, the transfer function $T(s)$ from input current $I(t)$ to the surface nominal surface concentration C_{ss}^j is given as

$$T(s) = \frac{C_{ss}^j}{I} = M^j \frac{\sinh(\sqrt{s\sigma_j^D})}{\sinh(\sqrt{s\sigma_j^D}) - \sqrt{s\sigma_j^D}\cosh\sqrt{s\sigma_j^D}} \quad (27)$$

Due to the advantages of Pade' approximation is that they naturally keeps the poles and zeros, this approximation method is applied to transfer function (27). The first order Pade' approximation is used, we have

$$T(s) \approx -M^j \frac{3/\sigma_j^D + \frac{2}{7}s}{s + \frac{\sigma_j^D}{35}s^2} \quad (28)$$

Then, the inverse laplace transform of (28) is implemented, one has

$$\ddot{c}_{ss}^j(t) = -\frac{35}{\sigma_j^D}\dot{c}_{ss}^j - \frac{105M^j}{(\sigma_j^D)^2}I(t) - \frac{10M^j}{\sigma_j^D}\dot{I}(t) \quad (29)$$

For the negative electrode, when the input current is constant($\dot{I} = 0$), then, the assumption of $\ddot{c}_{ss}^- = 0$ is reasonable. Hence, we have,

$$\dot{c}_{ss}^j(t) = \frac{3M^j}{(\sigma_j^D)}I(t) \quad (30)$$

For estimating the boundary state of negative electrode, designing the following boundary state estimator:

$$\begin{aligned} \dot{\hat{c}}_{ss}^-(t) &= \frac{3M^-}{(\sigma_j^D)}I(t) \\ &+L(\hat{V}(\hat{c}_{ss}^-(t),t) - V(c_{ss}^-(t),t)) \end{aligned} \quad (31)$$

where,

$$\begin{aligned} \hat{V}(\hat{c}_{ss}^-(t),t) &= \frac{RT}{\alpha F}\sinh^{-1}\left(\frac{-I(t)}{E^+\sqrt{\bar{c}_e\hat{c}_{ss}^+(c_{ss,max}^+ - \hat{c}_{ss}^+)}}\right) \\ &-\frac{RT}{\alpha F}\sinh^{-1}\left(\frac{I(t)}{E^-\sqrt{\bar{c}_e\hat{c}_{ss}^-(c_{ss,max}^- - \hat{c}_{ss}^-)}}\right) \\ &+U^+\left(\frac{\hat{c}_{ss}^+(t)}{c_{ss,max}^+}\right) - U^-\left(\frac{\hat{c}_{ss}^-(t)}{\hat{c}_{ss,max}^-(t)}\right) - R_f I(t) \\ &+R_e I(t) + K_f[\ln c_e(0^+,t) - \ln c_e(0^-,t)]. \end{aligned} \quad (32)$$

$$E^j = 2a^j L^j k^j \quad (33)$$

Theorem 1. The proposed boundary observer in equation (31) is stable if there is a gain L satisfying that $L > 0$.

Proof. Introducing the transformation $\tilde{c}_{ss}^-(t) = c_{ss}^-(t) - \hat{c}_{ss}^-(t)$ and subtracting (31) from (30), one has

$$\dot{\tilde{c}}_{ss}^-(t) = -L(\hat{V}(\hat{c}_{ss}^-(t),t) - V(c_{ss}^-(t),t)) \quad (34)$$

Using the following Lyapunov function:

$$V_L = \frac{1}{2\lambda}(\tilde{c}_{ss}^j)^2 \quad (35)$$

The time derivative of Lyapunov functional is obtained:

$$\begin{aligned} V_L &= \frac{1}{\lambda}\tilde{c}_{ss}^j\dot{\tilde{c}}_{ss}^j \\ &= -\frac{1}{\lambda}\tilde{c}_{ss}^j L(\hat{V}(\hat{c}_{ss}^-(t),t) - V) \end{aligned} \quad (36)$$

According to the monotonicity of $V(x_{ss}^-,t)$ with respect to x_{ss}^-, we have $sign(\tilde{x}_{ss}^-) = -sign(V(t) - \hat{V}(t))$. Then,

$$\tilde{x}_{ss}^- = -sign[V(t) - \hat{V}(t)] \times |\tilde{x}_{ss}^j| \quad (37)$$

Then,

$$\begin{aligned} V_L &= \frac{1}{\lambda}\tilde{c}_{ss}^j\dot{\tilde{c}}_{ss}^j \\ &= -\frac{1}{\lambda}L|\hat{V}(\hat{c}_{ss}^-(t),t) - V)| \times |\tilde{x}_{ss}^j| \\ &\le 0 \end{aligned} \quad (38)$$

4. THE LEAST SQUARES METHOD FOR CAPACITY ESTIMATION

Let $\tilde{c}_{ss,max}^- = c_{ss,max}^- - \hat{c}_{ss,max}^-, \tilde{c}_{ss,max}^+ = c_{ss,max}^+ - \hat{c}_{ss,max}^+$, then the terminal voltage can be rewritten as follows:

$$V(t) = \frac{RT}{\alpha F}\sinh^{-1}\left(\frac{-I(t)/E^{+}}{\sqrt{\bar{c}_e\hat{c}^{+}_{ss}(\hat{c}^{+}_{ss,max}+\tilde{c}^{+}_{ss,max}-\hat{c}^{+}_{ss})}}\right) - \frac{RT}{\alpha F}\sinh^{-1}\left(\frac{I(t)/E^{-}}{\sqrt{\bar{c}_e\hat{c}^{-}_{ss}(\hat{c}^{-}_{ss,max}+\tilde{c}^{-}_{ss,max}-\hat{c}^{-}_{ss})}}\right) + U^{+}\left(\frac{c^{+}_{ss}(t)}{\hat{c}^{+}_{ss,max}+\tilde{c}^{+}_{ss,max}}\right) - U^{-}\left(\frac{c^{-}_{ss}(t)}{\hat{c}^{-}_{ss,max}+\tilde{c}^{-}_{ss,max}}\right) - R_fI(t) + R_eI(t) + K_f[\ln c_e(0^{+},t) - \ln c_e(0^{-},t)]. \quad (39)$$

(39) is expanded by the McLaughlin series as follows:

$$V(t) = \frac{RT}{\alpha F}\sinh^{-1}\left(\frac{-I(t)/E^{+}}{\sqrt{\bar{c}_e\hat{c}^{+}_{ss}(\hat{c}^{+}_{ss,max}-\hat{c}^{+}_{ss})}}\right) - \frac{RT}{\alpha F}\sinh^{-1}\left(\frac{I(t)/E^{-}}{\sqrt{\bar{c}_e\hat{c}^{-}_{ss}(\hat{c}^{-}_{ss,max}-\hat{c}^{-}_{ss})}}\right) + U^{+}\left(\frac{c^{+}_{ss}(t)}{\hat{c}^{+}_{ss,max}}\right) - U^{-}\left(\frac{c^{-}_{ss}(t)}{\hat{c}^{-}_{ss,max}}\right) - R_fI(t) + R_eI(t) + K_f[\ln c_e(0^{+},t) - \ln c_e(0^{-},t)] + \frac{\partial V(c^{-}_{ss,max},t)}{\partial c^{-}_{ss,max}}\tilde{c}^{-}_{ss,max} + \Delta(c^{-}_{ss,max}). \quad (40)$$

where, $\Delta(c^{-}_{ss,max})$ is infinitesimal of higher order respect to $c^{-}_{ss,max}$.
Hence,

$$V(c^{-}_{ss,max}) - V(\hat{c}^{-}_{ss,max}) = \frac{\partial V(\hat{c}^{-}_{ss,max},t)}{\partial c^{-}_{ss,max}}\tilde{c}^{-}_{ss,max}. \quad (41)$$

where,

$$\hat{V}(\hat{c}^{-}_{ss,max}) = \frac{RT}{\alpha F}\sinh^{-1}\left(\frac{-I(t)/E^{+}}{\sqrt{\bar{c}_e\hat{c}^{+}_{ss}(\hat{c}^{+}_{ss,max}-\hat{c}^{+}_{ss})}}\right) - \frac{RT}{\alpha F}\sinh^{-1}\left(\frac{I(t)/E^{-}}{\sqrt{\bar{c}_e\hat{c}^{-}_{ss}(\hat{c}^{-}_{ss,max}-\hat{c}^{-}_{ss})}}\right) + U^{+}\left(\frac{c^{+}_{ss}(t)}{\hat{c}^{+}_{ss,max}}\right) - U^{-}\left(\frac{c^{-}_{ss}(t)}{\hat{c}^{-}_{ss,max}}\right) - R_fI(t) + R_eI(t) + K_f[\ln c_e(0^{+},t) - \ln c_e(0^{-},t)] \quad (42)$$

The least squares capacity estimation law is designed as follows

$$\dot{\hat{c}}^{-}_{ss,max} = -P\frac{\partial V(\hat{c}^{-}_{ss,max},t)}{\partial c^{-}_{ss,max}}(V(c^{-}_{ss,max}) - V(\hat{c}^{-}_{ss,max})) \quad (43)$$

where, P is a positive scalar. Using Lyapunov functional $\frac{1}{2}(\tilde{c}^{-}_{ss,max})^2$ can easily prove the exponential stability of $\tilde{c}^{-}_{ss,max}$ by estimation law (43).

5. SIMULATION RESULTS

The model parameters of electrochemical model are obtained from the paper [Forman et al.(2011)]. The true initial maximum lithium-ion concentration of anode is $29480 mol/m^3$ and the initial estimation lithium-ion concentration is set to $32000 mol/m^3$. Besides that, the true initial state of anode is $20000 mol/m^3$ and the initial estimation boundary value is $16000 mol/m^3$. We assume that the total number of lithium ions of anode is equal to that one of cathode which means that $\varepsilon^{-}c^{-}_{ss,max}L^{-} = \varepsilon^{+}c^{+}_{ss,max}L^{+}$. Hence, the maximum lithium-ion concentration of cathode can be obtained through the estimation of lithium-ion concentration in anode.

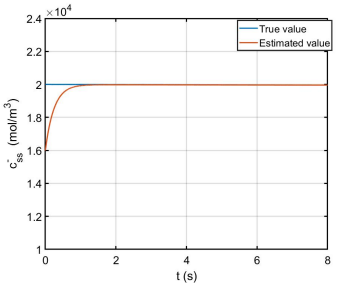

Fig. 2. The true boundary lithium-ion concentration and its estimation value

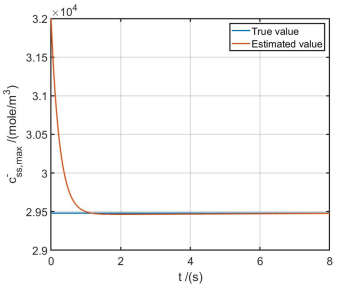

Fig. 3. The true maximum lithium-ion concentration and its estimation value

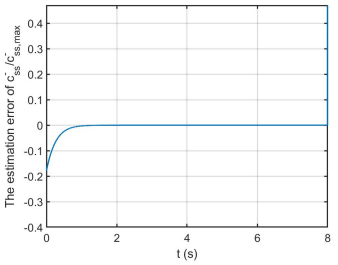

Fig. 4. The estimation error of c^{-}_{ss}/c^{-}_{ss}

In this simulation, 2C constant current is applied. Within 8 seconds, the estimation value of boundary lithium-ion concentration converges to the true one quickly as shown in Fig. 2. Fig. 3 presents the true maximum concentration and the estimation maximum concentration. Similar with Fig. 2, the estimation of the maximum lithium-ion concentration can approach to the true one fast. The result of Fig. 4 is consistent with those expressed in Fig. 2 and Fig. 3. Fig. 5 describes the error between the true terminal voltage and the estimation voltage. When both the estimation of boundary lithium-ion concentration and maximum lithium-ion concentration are close to the true value, the estimation of terminal voltage is also approximated to the true one.

6. CONCLUSION

In this paper, an electrochemical model considering the electrolyte dynamics is proposed to estimate the real capacity of a lithium-ion battery. Furthermore, a Pade' one-order approximation is adopted to obtain the transfer function between the boundary lithium-ion concentration

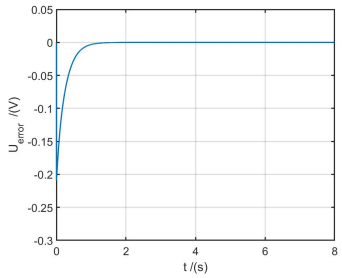

Fig. 5. The error between true terminal voltage and its estimation value

and input current, then a boundary state estimator is proposed to estimate the boundary lithium-ion concentration. Finally, the least square method is used to obtain the adaptive update law for maximum concentration estimation in anode.

REFERENCES

[Einhorn et al.(2012)] M. Einhorn et al. A Method for Online Capacity Estimation of Lithium Ion Battery Cells Using the State of Charge and the Transferred Charge. *IEEE Transactions on Industry Applications*, volume 48, (2), pages 736–741, 2012.

[Marongiu et al.(2016)] A. Marongiu et al. On-board capacity estimation of lithium iron phosphate batteries by means of half-cell curves. *Journal of Power Sources*, volume 324, pages 158–169, 2016.

[Fleischer et al.(2014)] C. Fleischer et al. On-line adaptive battery impedance parameter and state estimation considering physical principles in reduced order equivalent circuit battery models. *Journal of Power Sources*, volume 260, pages 276–291, 2014.

[Zhang et al.(2019)] D. Zhang et al. Real-Time Capacity Estimation of Lithium-Ion Batteries Utilizing Thermal Dynamics. *IEEE Transactions on Control Systems Technology*, pages 1–9, 2019.

[Moura et al.(2014)] S. J. Moura, N. A. Chaturvedi and M. Krsti?. Adaptive partial differential equation observer for battery state-of-charge/state-of-health estimation via an electrochemical model. *Journal of Dynamic Systems, Measurement and Control, Transactions of the ASME*, volume 136, (1), pages 11015, 2014.

[Li et al.(2018)] J. Li et al. A single particle model with chemical/mechanical degradation physics for lithium ion battery State of Health (SOH) estimation. *Applied Energy*, volume 212, pages 1178–1190, 2018.

[Bizeray et al.(2019)] A. M. Bizeray et al. Identifiability and Parameter Estimation of the Single Particle Lithium-Ion Battery Model. *IEEE Transactions on Control Systems Technology*, volume 27, (5), pages 1862–1877, 2019.

[Samad et al.(2016)] N. A. Samad et al. Battery capacity fading estimation using a force-based incremental capacity analysis. *Journal of the Electrochemical Society*, volume 163, (8), pages A1584–A1594, 2016.

[Baghdadi et al.(2016)] I. Baghdadi et al. Chemical rate phenomenon approach applied to lithium battery capacity fade estimation. *Microelectronics Reliability*, volume 64, (64), pages 134–139, 2016.

[Hoog et al.(2017)] J. de Hoog et al. Combined cycling and calendar capacity fade modeling of a Nickel-Manganese-Cobalt Oxide Cell with real-life profile validation. *Applied Energy*, volume 200, pages 47–61, 2017.

[Goh et al.(2017)] T. Goh et al. Capacity estimation algorithm with a second-order differential voltage curve for Li-ion batteries with NMC cathodes. *Energy*, volume 135, pages 257–268, 2017.

[Guha et al.(2018)] A. Guha and A. Patra. State of Health Estimation of Lithium-Ion Batteries Using Capacity Fade and Internal Resistance Growth Models. *IEEE Transactions on Transportation Electrification*, volume 4, (1), pages 135–146, 2018.

[Singh et al.(2019)] P. Singh et al. Semi-Empirical Capacity Fading Model for SoH Estimation of Li-Ion Batteries. *Applied Sciences*, volume 9, (15), pages 3012, 2019.

[Klass et al.(2012)] V. Klass et al. Evaluating Real-Life Performance of Lithium-Ion Battery Packs in Electric Vehicles. *Journal of the Electrochemical Society*, volume 159, (11), pages A1856–A1860, 2012.

[Kim et al.(2015)] T. Kim et al. A Rayleigh Quotient-Based Recursive Total-Least-Squares Online Maximum Capacity Estimation for Lithium-Ion Batteries. *IEEE Transactions on Energy Conversion*, volume 30, (3), pages 842–851, 2015.

[Hussein et al.(2015)] A. A. Hussein. Capacity Fade Estimation in Electric Vehicle Li-Ion Batteries Using Artificial Neural Networks. *IEEE Transactions on Industry Applications*, volume 51, (3), pages 2321–2330, 2015.

[Hu et al.(2015)] C. Hu et al. Online estimation of lithium-ion battery capacity using sparse Bayesian learning. *Journal of Power Sources*, volume 289, pages 105–113, 2015.

[Sung et al.(2016)] W. Sung et al. Robust and efficient capacity estimation using data-driven metamodel applicable to battery management system of electric vehicles. *Journal of the Electrochemical Society*, volume 163, (6), pages A981–A991, 2016.

[Liu et al.(2018)] Liu, Mingfang , et al. Modeling and numerical simulation of the battery capacity estimation based on neural network. *Modern Physics Letters B 32.34n36(2018)*.

[Richardson et al.(2019)] R. R. Richardson et al. Gaussian Process Regression for In Situ Capacity Estimation of Lithium-Ion Batteries. *IEEE Transactions on Industrial Informatics*, volume 15, (1), pages 127–138, 2019.

[Choi et al.(2019)] Y. Choi et al. Machine Learning-Based Lithium-Ion Battery Capacity Estimation Exploiting Multi-Channel Charging Profiles. *IEEE Access*, volume 7, pages 75143–75152, 2019.

[Forman et al.(2011)] J. C. Forman et al. Genetic parameter identification of the doyle-fuller-newman model from experimental cycling of a LiFePO4 battery. in 2011, .DOI: 10.1109/ACC.2011.5991183.